

Fundamental Properties of Full-Duplex Radio for Secure Wireless Communications

Yingbo Hua, Qiping Zhu, Reza Sohrabi

Abstract—This paper presents a number of fundamental properties of full-duplex radio for secure wireless communication under some simple and practical conditions. In particular, we consider the fields of secrecy capacity of a wireless channel between two single-antenna radios (Alice and Bob) against an unknown number of single-antenna eavesdroppers (Eves) from unknown locations, where Alice and Bob have zero knowledge (except a model) of the large-scale-fading channel-state-information of Eves. These properties show how the secrecy capacity is distributed in terms of the location of any Eve, how the optimal jamming power applied by the full-duplex radio varies with various parameters, and how bad or good the worst cases are. In particular, these properties show how the quality of self-interference cancellation/suppression affects various aspects of the fields of secrecy capacity. The cases of colluding Eves and non-colluding Eves are treated separately and yet coherently. For non-colluding Eves, asymptotically constant fields of secrecy capacity are revealed. For each of the two cases, we also treat subcases with or without small-scale fading.

I. INTRODUCTION

Wireless communication¹ is already firmly embedded in people’s lives around the world. Secure wireless communication is important for all of us from individuals and families to institutions and governments. Yet, the physical medium for wireless communication is intrinsically open to all wireless devices in any given space, time and bandwidth. This makes wireless communication particularly vulnerable to eavesdropping.

For secure communication, cryptography at the network and upper layers is an efficient, effective and indispensable tool [1]. Cryptography also makes wireless communication highly secure against eavesdropping as long as secret keys are kept secure and renewed frequently. However, when a secret key itself is distributed through wireless channels, the physical layer security becomes essential for secure wireless communications. A recent survey on physical layer security is available in [2], and a more general survey on wireless security is shown in [3].

The authors are with Department of Electrical and Computer Engineering, University of California, Riverside, CA 92521, USA. Emails: yhua@ece.ucr.edu; qzhu005@ucr.edu; and rsohr001@ucr.edu. This work was partially presented in a Keynote at the Full-Duplex Technology Workshop of IEEE PIMRC-2017, Montreal, Canada, Oct 10, 2017. The research was supported in part by the Army Research Office under Grant Number W911NF-17-1-0581. The views and conclusions contained in this document are those of the authors and should not be interpreted as representing the official policies, either expressed or implied, of the Army Research Office or the U.S. Government. The U.S. Government is authorized to reproduce and distribute reprints for Government purposes notwithstanding any copyright notation herein.

¹“Wireless communication” and “wireless communications” are considered interchangeable.

In this paper, we are interested in physical layer security via the use of full-duplex radio. A full-duplex radio is able to transmit and receive at the same time and same frequency, which differs from the conventional radio which only transmits and receives, respectively, in two separate time slots or at two separate frequencies. While research continues in order to improve the quality of full-duplex radio, prototypes of full-duplex radio can be found in [4] and the references therein.

A full-duplex radio is uniquely equipped for secure wireless communication. As a full-duplex radio receives a secret key from another radio, it can also transmit jamming noise² at the same time and same frequency to prevent eavesdroppers (Eves) from receiving the same key. It is this intrinsic characteristic of full-duplex radio that has recently drawn much interest in exploiting full-duplex radio for secure wireless communication. Such examples include fast power allocation for both a transmitter and a jamming receiver in a multicarrier setting [5], utilization of full-duplex for secure decentralized wireless network [6], resource allocation [7] and a hierarchical game [8] against an active full-duplex Eve [8], optimal power allocation for a multiuser MISO network against multiple Eves [9], and an early effort where MIMO full-duplex is exploited [10]. Many more relevant works can be found from the references therein.

However, a common assumption made in all these prior works is that the legitimate radios (such as Alice and Bob) know exactly how many Eves are nearby and also the large-scale-fading channel-state-information (L-CSI) of all Eves. This assumption is difficult to justify. If an Eve is passive and hidden (as it is often the case), it is virtually impossible for another radio to know its presence and let alone its L-CSI. Even if an Eve is active, its L-CSI is still hard to estimate without knowing either its location or its transmitted power. In other words, for most realistic situations, there is no way for a legitimate radio to know how many Eves are nearby, where they are, or what their L-CSI is.

In this paper, we focus on two basic schemes for key distribution (or any secret information³) between two single-antenna radios (called Alice and Bob) in the presence of single-antenna Eves, where we do not assume that Alice and Bob have any knowledge of the number of Eves, their locations or their L-CSI. We will adopt a reasonable model of L-CSI to map between L-CSI of any possible Eve and its approximate location. For small-scale-fading channel-state-information (S-

²The idea of using radio jamming to prevent adversaries from receiving secret information dates back at least to the era of World War II.

³If jamming is mainly used for exchange of secret keys, it would not overly interfere the rest of the network.

CSI), we will use the Rayleigh-amplitude statistical model as is commonly used and well justified for scattering-rich mobile environment. Based on the above models, we will study the field of the secrecy capacity of Alice and Bob, which is a function of the location of Eve. If the field is positive everywhere in the space where Eves could reside, then there is a positive secrecy capacity against any and all Eves in the space.

The primary findings of this work will be highlighted in a list of properties and, where effective, by illustrative figures. Some of these properties may be more important than others, some may be more surprising than others, and some of the proofs may be more straightforward than others. But we feel that they all provide fundamental insights into how the secrecy capacity of the studied system is distributed in terms of the (unknown) location of Eve, what and where the worst cases are, and how the jamming power from a full-duplex radio and the quality of its self-interference cancellation/suppression affect the fields of secrecy capacity.

This paper should be easy to read since the mathematical tools used in this paper are little more than what a college-level training in mathematics and statistics provides for engineering students. All proofs that are tedious manipulations are omitted. But for all results, we will at least provide the right directions (if not obvious) for readers to verify by themselves.

For the rest of this paper, we will start with mathematical normalization of the problem in section II where we remove all redundant variables that are easy to deal with whenever needed. We will treat the case of colluding Eves in section III and the case of non-colluding Eves in section IV. The work in section III is also very much coherent with that in section IV although the two cases are totally different scenarios in applications. In each of the two sections, we first handle the situation without small-scale fading and then the situation with small-scale fading. The final remarks are given in section V.

II. MATHEMATICAL NORMALIZATION

If Alice uses the power P'_T to transmit a key to Bob, and Bob (a full-duplex radio) receives the key and also sends out a jamming noise of the power P'_J , then the channel capacity⁴ from Alice to Bob usable for the packet of the key is known (e.g., see [11]) to be

$$C_{A,B} = \log_2(1 + SNR_{A,B}) \quad (1)$$

with $SNR_{A,B} = \frac{g'P'_T}{P'_{N,B} + \rho'P'_J}$ where g' is the squared amplitude of the (actual) channel gain from Alice to Bob, $P'_{N,B}$ is the (actual) variance of the background noise at Bob, and ρ' is the squared amplitude of the (actual) residual self-interference (SI) channel gain of Bob. The residual SI channel gain results from a combined effect of SI suppression at all stages, including antenna SI isolation, radio-frequency front-end SI cancellation and baseband SI cancellation. For principles of SI cancellation, see [12], for example, and the references therein.

⁴All capacity expressions in this paper have the unit in bits per channel use or equivalently in bits per second per Hertz.

At the same time, the channel capacity from Alice to Eve is

$$C_{A,E} = \log_2(1 + SNR_{A,E}) \quad (2)$$

with $SNR_{A,E} = \frac{a'P'_T}{P'_{N,E} + b'P'_J}$ where a' is the squared amplitude of the (actual) channel gain from Alice to Eve, b' is the squared amplitude of the (actual) channel gain from Bob to Eve, and $P'_{N,E}$ is the (actual) variance of the background noise at Eve.

To remove all redundant variables, we will use the following normalized variables: $P_T \doteq \frac{g'P'_T}{P'_{N,B}}$, $P_J \doteq \frac{g'P'_J}{P'_{N,B}}$, $\rho \doteq \frac{\rho'}{g'}$, $a \doteq \frac{a'P'_{N,B}}{g'P'_{N,E}}$ and $b \doteq \frac{b'P'_{N,B}}{g'P'_{N,E}}$, which are uniquely corresponding to P'_T , P'_J , ρ' , a' and b' , respectively, as long as Alice and Bob know the actual channel gain between them and the actual noise variances at all nodes. For convenience, we will assume that the variance of the background noise⁵ is the same for all nodes.

With the normalized variables, we can rewrite SNRs in (1) and (2) as follows⁶:

$$SNR_{A,B} = \frac{P_T}{1 + \rho P_J} \quad (3)$$

$$SNR_{A,E} = \frac{a P_T}{1 + b P_J} \quad (4)$$

We will use the expressions of (3) and (4) for the case without small-scale fading. In the case with small-scale fading, we will make modifications later.

Because of the above normalization, we will use the following terminology without loss of generality:

- 1) The distance between Alice and Bob is one, and the large-scale fading gain between them is one. Both nodes are located on the x -axis of a two-dimensional plane⁷: Alice is at $(-0.5, 0)$, and Bob is at $(0.5, 0)$. Eve's location is denoted by (x, y) . See Fig. 1.
- 2) The large-scale fading factor from Alice to Eve is denoted by $a = \frac{1}{d_A^\alpha}$ with $d_A = \sqrt{(x + 0.5)^2 + y^2}$, and the large-scale fading factor from Bob to Eve is denoted by $b = \frac{1}{d_B^\alpha}$ with $d_B = \sqrt{(x - 0.5)^2 + y^2}$. Here, $\alpha \geq 2$ is the path loss exponent.
- 3) The residual SI channel gain⁸ of a full-duplex radio is ρ . If $\rho (= \frac{\rho'}{g'})$ is less than one, it means that the actual amount of self-interference suppression used in the full-duplex radio is more than the large-scale path loss from Alice to Bob. It is important to remember that for a full-duplex radio with a fixed and actual residual SI channel gain ρ' , ρ can be larger or smaller than one depending on the actual channel gain g' between Alice and Bob.
- 4) The transmitted power⁹ from Alice is $P_T > 0$. The jamming power from Bob is $P_J \geq 0$. And the noise variance at all nodes is one.

⁵which includes thermal noise from within the device and radio noise from numerous sources of both man-made and nature-made

⁶With zero impact on reading, we will choose to ignore adding the period “.” at the end of an equation line that is also the end of a sentence.

⁷There is no loss of generality here since the 2-D results in this paper can be easily mapped into the 3-D space by a rotation around the x -axis.

⁸For convenience, we will also refer to “squared amplitude of channel gain” as “channel gain” unless clarification is needed.

⁹We assume that P_T is strictly larger than zero because if $P_T = 0$ there would be no transmission of information.

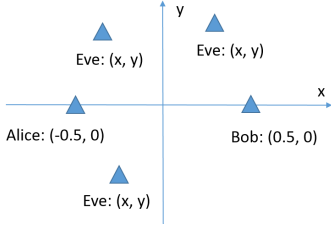


Fig. 1. Normalized coordinates.

The rest of this paper is divided into two cases: colluding Eves and non-colluding Eves. For each case, we also consider two subcases with or without small-scale fading.

III. WITH COLLUSION AMONG EAVESDROPPERS

We do not need to assume that Alice or Bob knows the number of Eves or the locations of Eves. But in this section, we assume that there could be collusion among all Eves at unknown locations. This means that if one Eve at one location steals a key, then all other Eves at any locations may also know the key.

A. Without small-scale fading

The secrecy capacity of the channel from Alice to Bob against Eve at location (x, y) is known (e.g., see [2]) to be

$$S_{A,B,x,y} = [C_{A,B} - C_{A,E}]^+ \quad (5)$$

where $(x)^+ = \max\{0, x\}$. Then, the secrecy capacity of the channel against all possible Eves is obviously the worst case:

$$S_{A,B} = \min_{x,y} S_{A,B,x,y} \quad (6)$$

We will see that without any constraint on (x, y) , $S_{A,B}$ would be always zero. However, it is practical to assume¹⁰ that there is a radius Δ around Alice within which there is no Eve. Naturally, this radius could be small or large, depending on applications. Hence, we will define the secrecy capacity in this case as

$$S_{A,B} = \min_{x,y,d_A \geq \Delta} S_{A,B,x,y} \quad (7)$$

In order to understand this secrecy capacity, it is sufficient to understand how $S_{A,B,x,y}$ is distributed in terms of (x, y) , which is studied next.

Define a SNR ratio:

$$\lambda_{x,y} \doteq \frac{SNR_{A,B}}{SNR_{A,E}} = \frac{1 + bP_J}{a(1 + \rho P_J)} \quad (8)$$

Obviously, $S_{x,y} > 0$ iff (if and only if) $\lambda_{x,y} > 1$. In terms of $\lambda_{x,y}$, $S_{A,B,x,y}$ has the following expression:

$$S_{A,B,x,y} = \begin{cases} (\log_2 e) \left(1 - \frac{1}{\lambda_{x,y}}\right)^+ SNR_{A,B}, & P_T \rightarrow 0 \\ (\log_2 \lambda_{x,y})^+, & P_T \rightarrow \infty \end{cases} \quad (9)$$

¹⁰Strictly speaking, this is a tiny amount of CSI about Eves. But this is negligible compared to the conventional definition of CSI.

The following property shows a deeper insight into the conditions under which the secrecy¹¹ $S_{A,B,x,y}$ is positive.

Property 1: Let $\gamma = \frac{a-1}{b-\rho a}$. Then, $S_{A,B,x,y} > 0$ iff

- 1) $b - \rho a > 0$ and $P_J > \gamma$; or
- 2) $b - \rho a < 0$ and $P_J < \gamma$; or
- 3) $b - \rho a = 0$ and $a < 1$.

Proof: The proof is straightforward based on the statement following (8). ■

The condition $b - \rho a > 0$ means that ρ must be small enough for the given a and b while $b - \rho a < 0$ requires ρ to be large enough. Keep in mind that both a and b are strictly positive and depend on Eve's location (x, y) . Also, iff $a > 1$, $d_A < 1$ (Eve is inside the unit circle around Alice); and iff $b < 1$, $d_B > 1$ (Eve is outside the unit circle around Bob). In order to view Property 1 geometrically, let us define the following four regions:

- 1) Region \mathcal{R}_1 : $b - \rho a > 0$ and $a < 1$.
- 2) Region \mathcal{R}_2 : $b - \rho a > 0$ and $a \geq 1$.
- 3) Region \mathcal{R}_3 : $b - \rho a \leq 0$ and $a < 1$. This region vanishes¹² iff $\rho \leq \frac{1}{2\alpha}$.
- 4) Region \mathcal{R}_4 : $b - \rho a \leq 0$ and $a \geq 1$.

Then, Property 1 implies:

Property 2:

- 1) If $(x, y) \in \mathcal{R}_1$, then $S_{A,B,x,y} > 0$ for any $P_J \geq 0$.
- 2) If $(x, y) \in \mathcal{R}_2$, then $S_{A,B,x,y} > 0$ iff $P_J > \gamma$.
- 3) If $(x, y) \in \mathcal{R}_3$, then $S_{A,B,x,y} > 0$ if $P_J = 0$.
- 4) If $(x, y) \in \mathcal{R}_4$, then $S_{A,B,x,y} = 0$ for any $P_J \geq 0$.

Proof: It follows from Property 1. ■

For \mathcal{R}_3 , it will be shown later that $\arg \max_{P_J} S_{A,B,x,y} = 0$, i.e., $P_J = 0$ is optimal. We see that unless Eve is in \mathcal{R}_4 , there is $P_J \geq 0$ such that $S_{A,B,x,y}$ is positive. Therefore, in order to have an overall positive secrecy, i.e., $S_{A,B} > 0$, it is necessary that $\mathcal{R}_4 \subset \mathcal{R}_{d_A < \Delta}$ (i.e., \mathcal{R}_4 belongs to the region where $d_A < \Delta$). One can verify that for $\Delta \leq 1$, $\mathcal{R}_4 \subset \mathcal{R}_{d_A < \Delta}$ iff $\rho < \frac{\Delta^\alpha}{(1+\Delta)^\alpha}$. (Note that if $\Delta > 1$, then by definition of \mathcal{R}_4 , $\mathcal{R}_4 \subset \mathcal{R}_{d_A \leq 1}$ as always, and hence $\mathcal{R}_4 \subset \mathcal{R}_{d_A < \Delta}$ for any ρ .) For example, if $\Delta = 0.1$ and $\alpha = 2$, then we need $\rho < 0.008 \approx -21\text{dB}$ (i.e., SI suppression needs to be 21dB more than the path loss from Alice to Bob).

In order to visualize Property 2, we need to visualize the region \mathcal{R}_ρ defined by $b - \rho a > 0$:

Property 3:

- 1) If $\rho = 1$, then $b - \rho a > 0$ is equivalent to $x > 0$.
- 2) If $\rho < 1$, then $b - \rho a > 0$ is equivalent to

$$(x + x_0)^2 + y^2 > r_\rho^2 \quad (10)$$

with $x_0 = \frac{1+\rho\frac{2}{\alpha}}{2(1-\rho\frac{2}{\alpha})} > \frac{1}{2}$ and $r_\rho = \sqrt{x_0^2 - \frac{1}{4}}$. That is, \mathcal{R}_ρ is everywhere outside a circular disk in the left half plane, and Alice is inside the disk.

- 3) If $\rho > 1$, then $b - \rho a > 0$ is equivalent to

$$(x + x_0)^2 + y^2 < r_\rho^2 \quad (11)$$

which means that \mathcal{R}_ρ is now everywhere inside a circular disk in the right half plane, and Bob is inside this disk.

¹¹For convenience, secrecy capacity is also referred to as secrecy.

¹²i.e., the two inequalities do not hold at the same time.

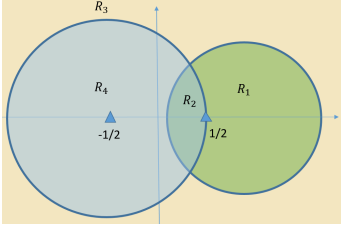


Fig. 2. Illustration of $\mathcal{R}_1, \mathcal{R}_2, \mathcal{R}_3$ and \mathcal{R}_4 for $\rho > 1$.

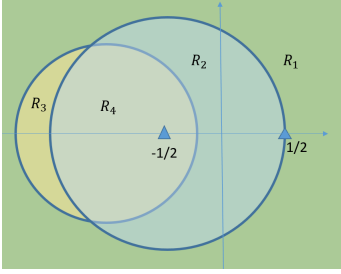


Fig. 3. Illustration of $\mathcal{R}_1, \mathcal{R}_2, \mathcal{R}_3$ and \mathcal{R}_4 for $\rho < 1$. \mathcal{R}_3 vanishes iff $\rho < \frac{1}{2\alpha}$.

Proof: The proof is straightforward. ■

The four regions $\mathcal{R}_1, \mathcal{R}_2, \mathcal{R}_3$ and \mathcal{R}_4 are illustrated in Figs. 2-3. Illustrated in Fig. 4 is the case where \mathcal{R}_4 shrinks into $\mathcal{R}_{d_A < \Delta}$.

Property 4: Given $\rho < \frac{1}{2\alpha}$, $P_J > 0$ and $\mathcal{R}_{P_J} \doteq \{(x, y) \in \mathcal{R}_\rho | P_J \leq \gamma\}$, then $S_{A,B,x,y} = 0$ iff $(x, y) \in \mathcal{R}_4 \cup \mathcal{R}_{P_J}$.

Proof: Under $\rho < \frac{1}{2\alpha}$, $\mathcal{R}_4 \subset \mathcal{R}_{d_A < 1}$. If $(x, y) \in \mathcal{R}_4$, we know that $S_{A,B,x,y} = 0$. If $(x, y) \notin \mathcal{R}_4$ but $(x, y) \in \mathcal{R}_{P_J}$, then we must have $b - \rho a > 0$ and $a > 1$ so that $P_J \leq \gamma$, which implies by Property 1 that $S_{A,B,x,y} = 0$. If $(x, y) \notin \mathcal{R}_4 \cup \mathcal{R}_{P_J}$, then $S_{A,B,x,y} > 0$ by Property 2. ■

This property says that for a fixed $P_J > 0$, there is an additional ring outside \mathcal{R}_4 where $S_{A,B,x,y} = 0$. This ring diminishes as P_J becomes infinite.

Property 5:

- 1) Provided $S_{A,B,x,y} > 0$, $S_{A,B,x,y}$ decreases if a increases (Eve moves towards Alice) or b decreases (Eve moves away from Bob).
- 2) Let $\rho < \frac{\Delta^\alpha}{(1+\Delta)^\alpha}$ with $\Delta \leq 1$. Subject to $P_J > \gamma$,

$$(x^*, y^*) \doteq \arg \min_{(x,y) \in \mathcal{R}_{d_A \geq \Delta}} S_{A,B,x,y} = (-\Delta - 0.5, 0)$$

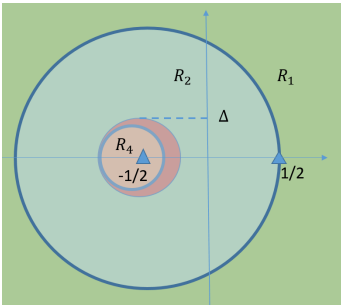


Fig. 4. Illustration of $\mathcal{R}_4 \subset \mathcal{R}_{d_A < \Delta}$ iff $\rho < \frac{\Delta^\alpha}{(1+\Delta)^\alpha}$ assuming $\Delta \leq 1$.

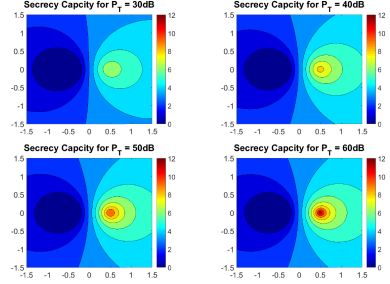


Fig. 5. $S_{A,B,x,y}$ vs (x, y) with $P_J = \sqrt{\frac{P_T}{\rho}}$, $\rho = 0.1$ and $\alpha = 2$. The darkest blue region is $\mathcal{R}_4 \cup \mathcal{R}_{P_J}$.

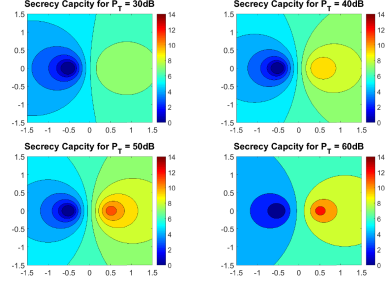


Fig. 6. $S_{A,B,x,y}$ vs (x, y) with $P_J = \sqrt{\frac{P_T}{\rho}}$, $\rho = 0.01$ and $\alpha = 2$. The darkest blue region is $\mathcal{R}_4 \cup \mathcal{R}_{P_J}$.

i.e., the most harmful location of Eve subject to $P_J > \gamma$ and $d_A \geq \Delta$ is at Δ distance to the left of Alice. Also note $(x^*, y^*) = \arg \max_{(x,y) \in \mathcal{R}_{d_A \geq \Delta}} C_{A,E} = \arg \min_{(x,y) \in \mathcal{R}_{d_A \geq \Delta}} \lambda_{x,y} = \arg \min_{(x,y) \in \mathcal{R}_{d_A \geq \Delta}} \frac{b}{a}$.

Proof: Part 1 is obvious from the definition of $S_{A,B,x,y}$ where $SNR_{A,B}$ is independent of a and b , and $SNR_{A,E}$ is an increasing function of a but a decreasing function of b . To prove Part 2, we first use Part 1 which suggests that for a fixed $a = \frac{1}{d_A}$, the minimum of $S_{A,B,x,y}$ is achieved by the smallest b which is $b = \frac{1}{(1+d_A)^\alpha}$. Then, subject to $d_A \geq \Delta$, $S_{A,B,x,y}$ is minimized by the above a and b with $d_A = \Delta$, which corresponds to $(x, y) = (-\Delta - 0.5, 0)$. ■

Shown in Figs. 5-6 is how $S_{A,B,x,y}$ is distributed over (x, y) subject to $P_J = \sqrt{\frac{P_T}{\rho}}$. We will see that the choice of $P_J = \sqrt{\frac{P_T}{\rho}}$ is an asymptotical form of the optimal jamming power. In these two figures, the secrecy $S_{A,B,x,y}$ is zero in $\mathcal{R}_4 \cup \mathcal{R}_{P_J}$ which is the darkest blue region. We see that $\mathcal{R}_4 \cup \mathcal{R}_{P_J}$ shrinks as ρ becomes smaller.

Property 6: Let $P_{J,opt,x,y} \doteq \arg \max_{P_J} S_{A,B,x,y}$. Then:

- 1) For $(x, y) \in \mathcal{R}_1$,

$$P_{J,opt,x,y} = \left[\gamma + \sqrt{\gamma^2 + \beta} \right]^+ \geq 0 \quad (12)$$

with $\gamma = \frac{a-1}{b-\rho a}$ and $\beta = \frac{ab-\rho+aP_T(b-\rho)}{\rho b(b-\rho a)}$.

- 2) For $(x, y) \in \mathcal{R}_2$, $P_{J,opt,x,y}$ is strictly positive and given by the equality in (12).
- 3) For $(x, y) \in \mathcal{R}_3$, $P_{J,opt,x,y} = 0$.

Proof: One can verify that if $S_{A,B,x,y} > 0$, then

$$\frac{\partial S_{A,B,x,y}}{\partial P_J} = \frac{(\log_2 e) P_T}{g(P_J)} (-c_2 P_J^2 + c_1 P_J + c_0) \quad (13)$$

where the numerator is a quadratic function of P_J and the denominator is always positive:

$$g(P_J) = (1+\rho P_J+P_T)(1+\rho P_J)(1+bP_J+aP_T)(1+bP_J) > 0 \quad (14)$$

and also

$$c_2 = \rho b(b - \rho a) \quad (15)$$

$$c_1 = 2\rho b(a - 1) \quad (16)$$

$$c_0 = ab - \rho + aP_T(b - \rho) \quad (17)$$

The stationary point of P_J at which $\frac{\partial S_{A,B,x,y}}{\partial P_J} = 0$ has obviously two possibilities: $\frac{c_1 \pm \sqrt{c_1^2 + 4c_0c_2}}{2c_2}$.

In region \mathcal{R}_1 where $b - \rho a > 0$ and $a < 1$, we have $c_2 > 0$ and $c_1 < 0$. But c_0 can be positive, zero or negative. If $c_0 > 0$, we see that $\frac{\partial S_{A,B,x,y}}{\partial P_J}$ is positive for small P_J and negative for large P_J , and hence $S_{A,B,x,y}$ must be maximized by

$$P_{J,opt,x,y} = \frac{c_1 + \sqrt{c_1^2 + 4c_0c_2}}{2c_2} = \gamma + \sqrt{\gamma^2 + \beta} > 0 \quad (18)$$

But if $c_0 \leq 0$, then $\frac{\partial S_{A,B,x,y}}{\partial P_J} < 0$ for all $P_J \geq 0$, and hence $S_{A,B,x,y}$ is maximized by $P_J = 0$.

In region \mathcal{R}_2 where $b - \rho a > 0$ and $a \geq 1$, we have $c_2 > 0$, $c_1 \geq 0$ and $c_0 > \frac{b}{a}[a^2 - 1 + aP_T(a - 1)] \geq 0$. In this case, we see that $\frac{\partial S_{A,B,x,y}}{\partial P_J}$ is positive for small P_J and negative for large P_J , and hence $S_{A,B,x,y}$ is maximized by the same P_J as shown in (18).

In region \mathcal{R}_3 where $b - \rho a \leq 0$ and $a < 1$, we have $c_2 \leq 0$, $c_1 < 0$ and $c_0 \leq \frac{b}{a}[a^2 - 1 + aP_T(a - 1)] < 0$, and hence $S_{A,B,x,y}$ is maximized by $P_J = 0$. ■

Recall that for region \mathcal{R}_4 , $S_{A,B,x,y} = 0$. So, only if $b - \rho a > 0$ (i.e., for $(x, y) \in \mathcal{R}_1 \cup \mathcal{R}_2$), P_J needs to be positive. Unless mentioned otherwise, we will assume $b - \rho a > 0$.

Obviously, with $b - \rho a > 0$, we have $\gamma > 0$ iff $a > 1$. And $\beta > 0$ if (not only if) $a > 1$. Also as $\rho \rightarrow 0$, γ becomes negligible compared to β , and hence $P_{J,opt,x,y} = \sqrt{\beta} = \sqrt{\frac{a(1+P_T)}{\rho b}}$. For Figs. 5 and 6, we have used this asymptotical form of $P_{J,opt,0,0}$ with large P_T , i.e., $P_J = \sqrt{\frac{P_T}{\rho}}$.

If we let $P_J = P_{J,opt,x,y}$, one can verify that

$$\lambda_{x,y} = \begin{cases} \sqrt{\frac{b}{\rho a}}, & P_T \rightarrow 0 \text{ and } \rho \rightarrow 0 \\ \frac{b}{\rho a}, & P_T \rightarrow \infty \end{cases} \quad (19)$$

The previous results of $P_{J,opt,x,y}$ depend on (x, y) , which are not directly useful. We need to know the worst case of $P_{J,opt,x,y}$.

Property 7: Subject to $(x, y) \in \mathcal{R}_2$, i.e., $b - \rho a > 0$ and $a \geq 1$:

- 1) As a increases (Eve moves towards Alice), both γ and β increase and hence $P_{J,opt,x,y}$ increases.
- 2) As b decreases (Eve moves away from Bob), both γ and β (although not as obvious) increases and hence $P_{J,opt,x,y}$ increases.
- 3) Subject to $d_A \geq \Delta$, $\arg \max_{x,y} P_{J,opt,x,y} = (x^*, y^*)$. In other words, when Eve is at (x^*, y^*) , not only the secrecy is minimum but also the optimal required jamming power is maximum.

Proof: Part 1 is obvious from (12). Part 2 for γ is also obvious. To prove the property of β in part 2, one can verify that

$$\frac{\partial \beta}{\partial b} = \frac{-a(1+P_T)b^2 + 2(1+aP_T)\rho b - a(1+aP_T)\rho^2}{\rho b^2(b-\rho a)^2} \quad (20)$$

where the numerator, denoted by $N(b)$, is upper bounded as follows:

$$\begin{aligned} N(b) &\leq \max_b N(b) = N(b)|_{b=\frac{(1+aP_T)\rho}{a(1+P_T)}} \\ &= \frac{\rho^2(1+aP_T)[(a^2-1) + a(a-1)P_T]}{a(1+P_T)} \leq 0 \end{aligned} \quad (21)$$

where the equality in the last inequality holds only for $a = 1$. The proof of part 3 is as follows. For a fixed $a = \frac{1}{d_A^\alpha}$, $\max_{b=1/d_B^\alpha} P_{J,opt,x,y}$ is achieved by $b = \frac{1}{(d_A+1)^\alpha}$ which is the minimum of b subject to $a = \frac{1}{d_A^\alpha}$. Furthermore, one can verify that subject to $a = \frac{1}{d_A^\alpha}$ and $b = \frac{1}{(d_A+1)^\alpha}$, both γ and β increase as d_A decreases. Hence, subject to $d_A \geq \Delta$, $\max_{x,y} P_{J,opt,x,y}$ is achieved by (x^*, y^*) . ■

An important implication of Property 7 is that if we know that Eves can only exist outside the disk $d_A < \Delta$, then the worst case in terms of both the secrecy $S_{A,B,x,y}$ and the optimal jamming power $P_{J,opt,x,y}$ is when Eve is at $(x^*, y^*) = (-\Delta - 0.5, 0)$, and the overall secrecy $S_{A,B}$ is optimized if we choose $P_J = P_{J,opt,x^*,y^*}$. Namely, the optimal value of $S_{A,B}$ is given by S_{A,B,x^*,y^*} with $P_J = P_{J,opt,x^*,y^*}$.

B. With small-scale fading

We now consider small-scale fading. In this case, the secrecy capacity $S_{A,B,x,y}$ is still given by (5) with (1) and (2). But the SNRs in (3) and (4) need to be revised as follows:

$$SNR_{A,B} = \frac{\tilde{A}P_T}{1 + \rho\tilde{B}P_J} \quad (22)$$

$$SNR_{A,E} = \frac{a\tilde{C}P_T}{1 + b\tilde{D}P_J} \quad (23)$$

where $\tilde{A}, \tilde{B}, \tilde{C}, \tilde{D}$ are small scale fading factors. We can assume that Alice and Bob know \tilde{A} and \tilde{B} but not \tilde{C} and \tilde{D} . In principle, Alice and Bob can make decisions based on the knowledge of \tilde{A} and \tilde{B} . Since the large-scale fading is already taken care of, we can assume that $\tilde{A}, \tilde{B}, \tilde{C}$ and \tilde{D} are i.i.d. (independent and identically distributed) and each has the exponential pdf (probability density function) e^{-u} with $u \geq 0$. Note that the amplitudes of all channel gains are proportional to the square-roots of these factors and hence are Rayleigh-distributed. Due to the random nature of \tilde{C} and \tilde{D} in particular, $S_{A,B,x,y}$ is now random. We will be interested in probabilities of zero secrecy and/or their upper bounds, which should be made small for good security.

We know that the secrecy $S_{A,B,x,y}$ is zero if and only if $SNR_{A,B} \leq SNR_{A,E}$ or equivalently,

$$\tilde{C} - v_1\tilde{D} - v_2 \geq 0 \quad (24)$$

with

$$v_1 = \frac{b\tilde{A}P_J}{a(1 + \rho\tilde{B}P_J)} \quad (25)$$

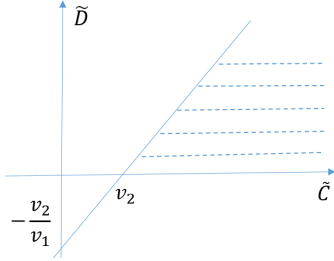


Fig. 7. The shaded region is defined by (24).

$$v_2 = \frac{\tilde{A}}{a(1 + \rho\tilde{B}P_J)} \quad (26)$$

Notice that if P_J increases, v_1 increases and v_2 decreases. The region defined by (24) is illustrated by the shaded area in Fig. 7.

Property 8:

- 1) The conditional probability of zero secrecy, conditional upon \tilde{A} and \tilde{B} , is

$$\begin{aligned} \mathcal{P}_{\{S_{A,B,x,y}=0|\tilde{A},\tilde{B}\}} &= \int_0^\infty dv \int_{v_1 v + v_2}^\infty e^{-u-v} du \\ &= \frac{e^{-v_2}}{1 + v_1} < \frac{1}{1 + v_1} \end{aligned} \quad (27)$$

- 2) Subject to $d_A \geq \Delta$, $\arg \max_{x,y} \mathcal{P}_{\{S_{A,B,x,y}=0|\tilde{A},\tilde{B}\}} = (x^*, y^*)$, i.e., the worst location of Eve is the same as shown before.
- 3) If Eve is arbitrarily close to Alice, the probability of zero secrecy is one, i.e., $\mathcal{P}_{\{S_{A,B,-0.5,0}=0|\tilde{A},\tilde{B}\}} = \mathcal{P}_{\{S_{A,B,-0.5,0}=0\}} = 1$.
- 4) In general, the unconditional probability of zero secrecy is:

$$\mathcal{P}_{\{S_{A,B,x,y}=0\}} = \mathcal{E}\{\mathcal{P}_{\{S_{A,B,x,y}=0|\tilde{A},\tilde{B}\}}\} < \mathcal{E}\left\{\frac{1}{1 + v_1}\right\} \quad (28)$$

where the upper bound is a decreasing function¹³ of P_J and is maximized when Eve is at (x^*, y^*) subject to $d_A \geq \Delta$.

Proof: For Part 1, we see that $\mathcal{P}_{\{S_{A,B,x,y}=0|\tilde{A},\tilde{B}\}}$ is equivalent to $\mathcal{P}_{\{\tilde{C}-v_1\tilde{D}-v_2 \geq 0\}}$ which equals the integral of the joint pdf of \tilde{C} and \tilde{D} over the shaded region shown in Fig. 7. For part 2, note that $\mathcal{P}_{\{S_{A,B,x,y}=0|\tilde{A},\tilde{B}\}}$ decreases as v_1 and/or v_2 increase, or equivalently, as a decreases and/or b increases. So, for a fixed $a = \frac{1}{d_A^\alpha}$, $\arg \max_b \mathcal{P}_{\{S_{A,B,x,y}=0|\tilde{A},\tilde{B}\}} = \arg \min_b v_1 = \frac{1}{(d_A+1)^\alpha}$. Then, subject to $a = \frac{1}{d_A^\alpha}$, $b = \frac{1}{(d_A+1)^\alpha}$ and $d_A \geq \Delta$, $\arg \max_{d_A} \mathcal{P}_{\{S_{A,B}=0|\tilde{A},\tilde{B}\}} = \arg \min_{d_A} v_1 = \arg \min_{d_A} v_2 = \Delta$. Part 3 follows by using $a = \infty$ and $b = 1$ (i.e., $v_1 = 0$ and $v_2 = 0$) in (27). Part 4 is obvious. ■

Although the optimal jamming power in terms of the upper bound (28) on the unconditional probability of zero secrecy $\mathcal{P}_{\{S_{A,B,x,y}=0\}}$ is infinite, it is not yet clear whether the optimal jamming power in terms of the conditional probability of zero

secrecy $\mathcal{P}_{\{S_{A,B,x,y}=0|\tilde{A},\tilde{B}\}}$ is also infinite. Keep in mind that the choice of P_J can be based on \tilde{A} and \tilde{B} which are known to Alice and Bob.

One can verify that

$$\begin{aligned} &\frac{\partial \mathcal{P}_{\{S_{A,B,x,y}=0|\tilde{A},\tilde{B}\}}}{\partial P_J} \\ &= \frac{-\tilde{A}e^{-v_2}(a_1 P_J + a_0)}{(a(1 + \rho\tilde{B}P_J) + b\tilde{A}P_J)^2(1 + \rho\tilde{B}P_J)} \end{aligned} \quad (29)$$

with $a_1 = \rho\tilde{B}[a(b-\rho\tilde{B})-b\tilde{A}]$ and $a_0 = a(b-\rho\tilde{B})$. We see that each of a_0 and a_1 can be either positive or negative. If $a_0 > 0$ and $a_1 > 0$, then $\mathcal{P}_{\{S_{A,B,x,y}=0|\tilde{A},\tilde{B}\}}$ is always a decreasing function of P_J and hence the optimal value $P_{J,opt,x,y}$ of P_J is infinite. If $a_0 > 0$ and $a_1 < 0$, then there is a finite optimal power, i.e., $P_{J,opt,x,y} = \frac{a_0}{-a_1}$. If $a_0 < 0$, which also implies $a_1 < 0$, then $\mathcal{P}_{\{S_{A,B,x,y}=0|\tilde{A},\tilde{B}\}}$ is always an increasing function of P_J , for which $P_{J,opt,x,y} = 0$.

We see that depending on the realizations of \tilde{A} and \tilde{B} , the optimal jamming power could be zero, finite or infinite. However, one can verify that the condition where $a_0 > 0$ and $a_1 > 0$ is equivalent to $\tilde{B} < \frac{b}{\rho}$ and $\tilde{A} < a(1 - \frac{\rho}{b}\tilde{B})$, which is also equivalent to $\tilde{A} < a$ and $\tilde{B} < \frac{b}{\rho}(1 - \frac{\tilde{A}}{a})$. This observation leads to:

Property 9:

- 1) A lower bound on the probability of $\mathcal{P}_{\{S_{A,B,x,y}=0|\tilde{A},\tilde{B}\}}$ being a decreasing function of P_J is:

$$\begin{aligned} &Prob\left\{\tilde{A} < a \text{ and } \tilde{B} < \frac{b}{\rho}\left(1 - \frac{\tilde{A}}{a}\right)\right\} \\ &= \int_0^a du \int_0^{\frac{b}{\rho}(1-\frac{u}{a})} e^{-u-v} dv \\ &= 1 - \frac{b}{b-\rho a}e^{-a} + \frac{\rho a}{b-\rho a}e^{-\frac{b}{\rho}} \doteq \underline{\mathcal{P}} \end{aligned} \quad (30)$$

- 2) Let $\frac{b}{\rho} = \eta a$ with $\eta > 1$. Then,

$$\underline{\mathcal{P}} = 1 - \frac{1}{\eta-1}[\eta e^{-a} - e^{-\eta a}] = \begin{cases} 1, & a = \infty \\ 1 - e^{-a}, & \eta = \infty \end{cases} \quad (31)$$

and $\underline{\mathcal{P}}$ increases rapidly to one as a increases for any $\eta > 1$.

Proof: The proof is straightforward. ■

For example, if $\Delta = 0.1$, $\alpha = 2$ and $\eta = 1.01$ (i.e., $\rho \approx -21$ dB), then at (x^*, y^*) , $\underline{\mathcal{P}} = 1 - 2.3 \times 10^{-42}$. This example suggests although in general the optimal jamming power may be finite depending on \tilde{A} and \tilde{B} , almost surely the (worst-case) conditional probability of zero secrecy is a decreasing function of P_J for which the optimal jamming power is infinite¹⁴.

Shown in Fig. 8 are the unconditional probability of zero secrecy $\mathcal{P}_{\{S_{A,B,x^*,y^*}=0\}}$ and its upper bound given by (28) with $\Delta = 0.1$, $\alpha = 2$ and $\eta = 1.01$. The gap of the bound is small (intuitively because of the small v_2 in e^{-v_2} in (27)). We see that $\mathcal{P}_{\{S_{A,B,x^*,y^*}=0\}}$ is about 0.5 for $P_J \geq 40$ dB. If we use 10 transmissions of 10 keys under independent small-scale fading, we could have the unconditional probability of

¹³Due to v_2 in (27), the monotonic property of the exact $\mathcal{P}_{\{S_{A,B,x,y}=0\}}$ in terms of P_J has so far no proof.

¹⁴In practice, this should be translated into a maximum allowed jamming power.

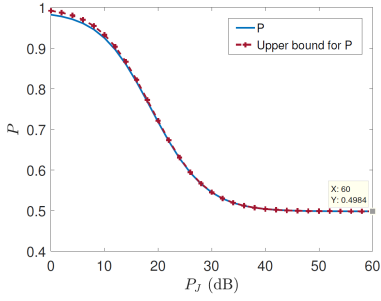


Fig. 8. $\mathcal{P}_{\{S_{A,B,x^*,y^*}=0\}}$ and its upper bound given by (28) with $\Delta = 0.1$, $\alpha = 2$ and $\eta = 1.01$ ($\rho = 21\text{dB}$).

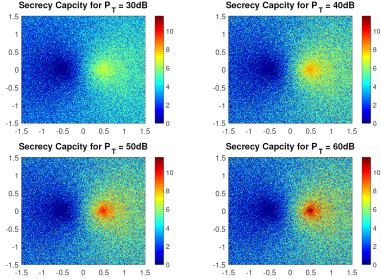


Fig. 9. With small-scale fading and subject to $\tilde{A} = \tilde{B} = 1$, $S_{A,B,x,y}$ versus (x, y) with $P_J = \sqrt{\frac{P_T}{\rho}}$, $\rho = 0.1$ and $\alpha = 2$.

zero secrecy guaranteed to be less than 2^{-10} everywhere subject to $d_A \geq 0.1$. Note that zero secrecy of the 10 transmissions happens iff each of the 10 transmissions has zero secrecy. In other words, if any of the transmissions has a positive secrecy, the overall secrecy is positive¹⁵. To achieve independent small-scale fading between transmissions in scattering-rich environments, Alice and Bob can simply move their locations by a short distance in the order of half-wavelength after each transmission.

Shown in Fig. 10 and 9 are examples of $S_{A,B,x,y}$ versus (x, y) with small-scale fading subject to $\tilde{A} = \tilde{B} = 1$. In these figures, the step size in each of x and y directions is 0.01. For each sample of (x, y) , an independent realization of \tilde{C} and \tilde{D} is used. We see that due to small-scale fading, even in region \mathcal{R}_4 the conditional probability of zero secrecy is not zero (unless $a = \infty$ or $d_A = 0$).

The conditional probability of zero secrecy $\mathcal{P}_{\{S_{A,B,x,y}=0|\tilde{A},\tilde{B}\}}$ in (27) can be used by Alice and Bob for opportunistic transmission of secret keys. In scattering-rich environment, \tilde{A} and \tilde{B} can change significantly after a small amount (in the order of half-wavelength) of location change of Bob. (Note that a location change of Alice would affect \tilde{A} , \tilde{C} and \tilde{D} significantly but likely do little for \tilde{B} . This is because the self-interference channel of Bob is mainly affected by objects around Bob.) In particular, for mobile ad hoc network (MANET), Alice and Bob could both move around until $\mathcal{P}_{\{S_{A,B,x,y}=0|\tilde{A},\tilde{B}\}}$ is small enough. Based on (25), (26) and (27), we see that $\mathcal{P}_{\{S_{A,B,x,y}=0|\tilde{A},\tilde{B}\}}$ is minimized by the largest \tilde{A} and the smallest \tilde{B} .

¹⁵In practice, one would need a bit of extra margin of a positive secrecy so that the security is reliable subject to unknown errors.

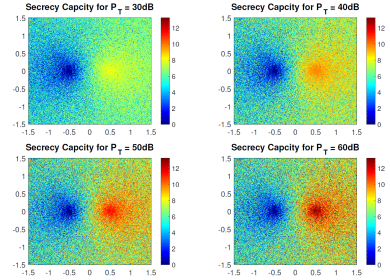


Fig. 10. With small-scale fading and subject to $\tilde{A} = \tilde{B} = 1$, $S_{A,B,x,y}$ versus (x, y) with $P_J = \sqrt{\frac{P_T}{\rho}}$, $\rho = 0.01$ and $\alpha = 2$.

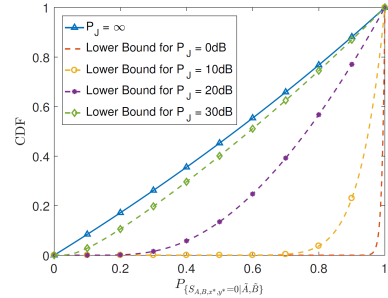


Fig. 11. Lower bound on CDF of $\mathcal{P}_{\{S_{A,B,x^*,y^*}=0|\tilde{A},\tilde{B}\}}$ with $\rho = 0.01$ and $(x^*, y^*) = (-\Delta - 0.5, 0) = (-0.6, 0)$.

For opportunistic transmission of secret keys, it is useful to consider the cumulative distribution function (CDF) of $\mathcal{P}_{\{S_{A,B,x,y}=0|\tilde{A},\tilde{B}\}}$ as well as its dependence on P_J . A closed-form CDF of the exact $\mathcal{P}_{\{S_{A,B,x,y}=0|\tilde{A},\tilde{B}\}}$ seems intractable to find. But using the upper bound in (27), one can verify the following lower bound on the CDF of $\mathcal{P}_{\{S_{A,B,x,y}=0|\tilde{A},\tilde{B}\}}$:

$$\begin{aligned} \mathcal{F}_{\{A,B,x,y\}}(p) &\doteq \text{Prob}\{\mathcal{P}_{\{S_{A,B,x,y}=0|\tilde{A},\tilde{B}\}} \leq p\} \\ &> \text{Prob}\left\{\frac{1}{1+v_1} \leq p\right\} \\ &= e^{-\frac{a(1-p)}{bP_J p}} \frac{bp}{bp + a\rho(1-p)} \end{aligned} \quad (32)$$

where $0 < p \leq 1$. A simple dependence of the lower bound of $\mathcal{F}_{\{A,B,x,y\}}(p)$ on P_J is very clear in (32). One can also verify that if $P_J = \infty$,

$$\mathcal{F}_{\{A,B,x,y\}}(p) = \frac{bp}{bp + a\rho(1-p)} \quad (33)$$

which means that the inequality in (32) becomes equality under $P_J = \infty$.

Shown in Fig. 11 is the CDF lower bound given by (32). For example, we see that at $P_J = 30\text{dB}$, there is at least a 10% chance (with respect to the random \tilde{A} and \tilde{B} that are known to Alice and Bob) that $\mathcal{P}_{\{S_{A,B,x^*,y^*}=0|\tilde{A},\tilde{B}\}} < 20\%$ (with respect to the random \tilde{C} and \tilde{D} that are unknown to Alice and Bob). In other words, for any given $0 < p < 1$, the larger is the CDF lower bound, the more likely can Alice and Bob encounter such \tilde{A} and \tilde{B} that the conditional probability of zero secrecy is less than p .

IV. WITHOUT COLLUSION AMONG EAVESDROPPERS

Now we consider the case where there is no collusion among Eves. Namely, all Eves act as isolated individuals. To reveal the fundamentals, we continue to assume the simple system discussed so far. But in this section, we also assume that Alice and Bob are both full-duplex radios and of equal characteristics in terms of P_T , P_J and ρ .

To take the advantage of no collusion among Eves, we consider a dual-phase transmission scheme. In phase 1, Alice first sends a random key K_1 to Bob while Bob receives the key and also jams Eves in full-duplex mode. In phase 2, Bob sends another random key K_2 to Alice as Alice receives the key and also jam Eves in full-duplex mode. Following the dual-phase scheme, each of the two nodes has the same pair of keys (K_1, K_2) as their secret information.

The above scheme was inspired by a scheme in [13] where a so-called iJam was proposed for conventional half-duplex radios. In phase 1 of iJam, Alice sends a random key K_1 over N subcarriers to Bob while Bob jams Eves over a random subset \mathcal{S}_1 of $\frac{N}{2}$ subcarriers and receives samples over the other subset \mathcal{S}_2 of $\frac{N}{2}$ subcarriers. Then, Alice repeats the same process while Bob jams Eves over \mathcal{S}_2 and receives samples over \mathcal{S}_1 . Combining the un-jammed samples received during the two transmissions in phase 1, Bob recovers K_1 . In phase 2 of iJam, the roles of Alice and Bob are reversed, and after two repeated transmissions from Bob, Alice receives another key K_2 from Bob.

To compare our scheme with iJam conveniently, we will call our scheme fJam. The main differences between fJam and iJam are:

- 1) For the same pair of keys, iJam could require up to twice as much spectral resource as fJam requires.
- 2) The header of each transmitted packet by iJam is not jammed and is completely transparent to Eves while fJam jams the entire packet of each transmission. It is important to note that the header of a packet also carries important information such as pilots for channel estimation.
- 3) A random \mathcal{S}_1 in iJam has a finite number $C_{\frac{N}{2}}^N = \frac{N!}{(\frac{N}{2}!)^2} < 2^N$ of possibilities. Under iJam, Eve is in theory able to recover both keys through exhaust search although the computational complexity is increased by $(C_{\frac{N}{2}}^N)^2$ times when compared to no jamming. In other words, the secrecy capacity of iJam is actually zero. But under fJam, the secrecy capacity can be easily made positive, and no Eve is even in theory able to recover both keys correctly with infinite computational power.

A. Without small-scale fading

As long as the time taken between the two phases is small enough, we can assume that the location and channel response of any Eve is unchanged. The secrecy capacity of fJam against Eve at unknown location (x, y) is therefore:

$$S_{x,y} = \frac{1}{2}(S_{A,B,x,y} + S_{B,A,x,y}) \quad (34)$$

with $S_{A,B,x,y} = (C_{A,B} - C_{A,E})^+$, $S_{B,A,x,y} = (C_{B,A} - C_{B,E})^+$, $C_{A,B} = \log_2(1 + SNR_{A,B})$, $C_{B,A} = \log_2(1 +$

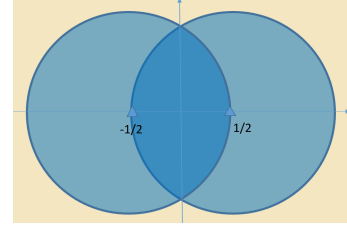


Fig. 12. With $P_J = 0$, $S_{x,y} > 0$ iff (x, y) is not in the dark blue region (i.e., the “almond-shaped” region).

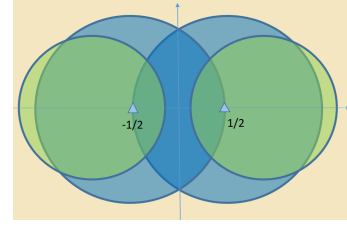


Fig. 13. “There is $P_J \geq 0$ such that $S_{x,y} > 0$ ” iff (x, y) is not in the dark blue region which vanishes iff $\rho < 1$.

$SNR_{B,A}$), $C_{A,E} = \log_2(1 + SNR_{A,E})$, $C_{B,E} = \log_2(1 + SNR_{B,E})$ and

$$SNR_{A,B} = SNR_{B,A} = \frac{P_T}{1 + \rho P_J} \doteq SNR \quad (35)$$

$$SNR_{A,E} = \frac{aP_T}{1 + bP_J} \quad (36)$$

$$SNR_{B,E} = \frac{bP_T}{1 + aP_J} \quad (37)$$

The overall secrecy capacity of fJam against all Eves should be $S = \min_{x,y} S_{x,y}$, which could also be subject to some constraint on (x, y) if there is any prior knowledge of the locations of Eves. Clearly, in order to understand S , it is sufficient to understand $S_{x,y}$ as a function of (x, y) . In particular, we are interested in the worst cases of $S_{x,y}$.

We see that $S_{x,y}$ is symmetric between a and b since it is an average of $S_{A,B,x,y}$ and $S_{B,A,x,y}$. Recall Property 2. There are four unique regions of $S_{A,B,x,y}$, i.e., \mathcal{R}_i with $i = 1, 2, 3, 4$, which can be rewritten as $\mathcal{R}_i = \mathcal{R}_i(a, b)$ to stress its dependence on a and b . Therefore, for $S_{B,A,x,y}$, there must be corresponding four regions which we can denote by $\bar{\mathcal{R}}_i$ with $i = 1, 2, 3, 4$, and $\bar{\mathcal{R}}_i = \mathcal{R}_i(b, a)$. Similarly, we will write $\mathcal{R}_\rho = \mathcal{R}_\rho(a, b)$ and $\bar{\mathcal{R}}_\rho = \mathcal{R}_\rho(b, a)$. Also, $\gamma = \gamma(a, b)$ and $\bar{\gamma} = \gamma(b, a)$. Therefore, we have:

Property 10:

- 1) If $P_J = 0$, then $S_{x,y} > 0$ iff $(x, y) \notin \mathcal{R}_{d_A \leq 1} \cap \mathcal{R}_{d_B \leq 1}$.
- 2) “There is $P_J \geq 0$ such that $S_{x,y} > 0$ ” iff $(x, y) \notin \mathcal{R}_4 \cap \bar{\mathcal{R}}_4$.
- 3) “For arbitrary (x, y) , there is $P_J \geq 0$ such that $S_{x,y} > 0$ ” iff $\rho < 1$.

Proof: The proof is easy based on Property 2. ■

Part 1 of Property 10 is illustrated in Fig. 12. Part 2 of Property 10 is illustrated in Fig. 13 with $\rho > 1$. Part 3 says that in order to have a positive secrecy against Eve at any location we must have $\rho < 1$. We will assume $\rho < 1$.

The general landscape of $S_{x,y}$ is a function of ρ , P_T and P_J , and is more complicated than that of $S_{A,B,x,y}$. In particular, unlike $S_{A,B,x,y}$, $S_{x,y}$ does not in general increase or decrease monotonically with respect to either a or b . But an important and tractable region of $S_{x,y}$ is along the x -axis and the y -axis, which will be focused on next.

Property 11: Assume $(x, y) \in \mathcal{R}_\rho \cap \bar{\mathcal{R}}_\rho$ and $P_J > \max\{\gamma, \bar{\gamma}\}$. Then, $S_{0,0}$ is the minimum of $S_{x,y}$ along the y -axis, and $S_{0,y}$ increases as $|y|$ increases.

Proof: It is easy to verify that under the stated condition,

$$S_{x,y} = \log_2(1 + SNR) - \frac{1}{2} \log_2 T_{x,y} \quad (38)$$

with

$$\begin{aligned} T_{x,y} &= (1 + SNR_{A,E})(1 + SNR_{B,E}) \\ &= \frac{(1 + bP_J + aP_T)(1 + aP_J + bP_T)}{(1 + bP_J)(1 + aP_J)} \end{aligned} \quad (39)$$

Let $x = 0$. Then, $a = b = \frac{1}{(0.25 + y^2)^{\alpha/2}}$ and $T_{0,y} = \left(1 + \frac{aP_T}{1 + aP_T}\right)^2$ which decreases as $|y|$ increases and has its maximum at $y = 0$. Hence, $S_{0,y}$ increases as $|y|$ increases and has its minimum at $y = 0$. ■

But along the x -axis, $S_{x,y}$ is no longer as monotonic as it is along the y -axis. The pattern of $S_{x,0}$ is highly sensitive to the choice of P_T and P_J :

Property 12: Assume $\rho < 1$ and $P_J > \frac{1 - 2^{-\alpha}}{1 - \rho}$. Then, $S_{0,0}$ is a local maximum along the x -axis if

$$P_J > \frac{-1 + \sqrt{1 + 2^{\alpha+1} P_T}}{2^{\alpha+1}} \quad (40)$$

If the inequality is reversed, $S_{0,0}$ is a local minimum along the x -axis.

Proof: The stated condition complies with that of Property 11 and hence (38) holds. One can verify that for $y = 0$ and a small $x \neq 0$,

$$\begin{aligned} T_{x,0} &= T_{0,0} + \\ &\frac{\alpha^2 2^{2(\alpha+1)}}{(1 + 2^\alpha P_J)^2} \left[\left(1 + \frac{2^\alpha P_T}{1 + 2^\alpha P_J}\right)^2 P_J^2 - (P_J - P_T)^2 \right] x^2 \end{aligned} \quad (41)$$

If $P_J \geq P_T$, (41) obviously implies that $T_{x,0} > T_{0,0}$ and hence $T_{0,0}$ ($S_{0,0}$) is a local minimum (maximum) along the x -axis. But more generally, $S_{0,0}$ is a local maximum along the x -axis if the coefficient of x^2 in (41) is positive. One can verify that this condition is equivalent to $2^{\alpha+1} P_J^2 + 2P_J - P_T > 0$ which is also equivalent to (40). The converse is obvious. ■

We now look deeper into $S_{x,0}$. For convenience, we let $d = a$, $a = \frac{1}{d^\alpha}$ and $b = \frac{1}{(1-d)^\alpha}$. Then $\log_2 T_{x,0} = \log_2 T_{d-0.5,0}$ which is a function of d with $d = x + 0.5$. Assuming the condition of Property 11, one can verify that¹⁶

$$\frac{\partial \log_2 S_{x,0}}{\partial x} = -\frac{1}{2} \frac{\partial \log_2 T_{x,0}}{\partial x} = -\frac{\log_2 e}{2} \frac{N(d)}{D(d)} \quad (42)$$

with

$$\begin{aligned} D(d) &= \left(1 + \frac{P_J}{(1-d)^\alpha} + \frac{P_T}{d^\alpha}\right) \left(1 + \frac{P_J}{(1-d)^\alpha}\right) \\ &\cdot \left(1 + \frac{P_J}{d^\alpha} + \frac{P_T}{(1-d)^\alpha}\right) \left(1 + \frac{P_J}{d^\alpha}\right) > 0 \end{aligned} \quad (43)$$

$$\begin{aligned} N(d) &= -\alpha P_J P_T^2 \frac{d^{\alpha-1} - (1-d)^{\alpha-1}}{d^{2\alpha} (1-d)^{2\alpha}} \\ &+ \alpha P_T \frac{d^{\alpha+1} - (1-d)^{\alpha+1}}{d^{\alpha+1} (1-d)^{\alpha+1}} + 2\alpha P_J P_T \frac{d^{2\alpha+1} - (1-d)^{2\alpha+1}}{d^{2\alpha+1} (1-d)^{2\alpha+1}} \\ &+ \alpha P_J^2 P_T \left(2 \frac{d^\alpha - (1-d)^\alpha}{d^{2\alpha+1} (1-d)^{2\alpha+1}} + \frac{d^{3\alpha+1} - (1-d)^{3\alpha+1}}{d^{3\alpha+1} (1-d)^{3\alpha+1}}\right) \\ &+ \alpha P_J^3 P_T \frac{d^{2\alpha} - (1-d)^{2\alpha}}{d^{3\alpha+1} (1-d)^{3\alpha+1}} + \alpha P_T^2 \frac{2d-1}{d^{\alpha+1} (1-d)^{\alpha+1}} \end{aligned} \quad (44)$$

Due to the symmetry $S_{x,0} = S_{-x,0}$, we only need to consider $x \geq 0$ (i.e., $d \geq 0.5$). We see that all terms in $N(d)$ are negative if $d > 1$. Hence, under the condition of Property 11, $S_{x,0}$ is an increasing function of x for $x > 0.5$. It is also interesting to see that if $1 > d > 0.5$, all terms in $N(d)$ except the first term are positive, and the first term is dominated by some other terms if P_J is large enough. So, if P_J is large enough, $S_{x,0}$ must be a decreasing function of x for $0 < x < 0.5$, which is consistent with Property 12.

Also note that all terms in $N(d)$ except the first term change their sign as d increases across the value of one. Furthermore, one can verify:

Property 13: Under the condition of Property 11, if we let $x \rightarrow 0.5$, then

$$\frac{\partial \log_2 S(x,0)}{\partial x} = -\frac{\log_2 e}{2} \frac{\alpha}{0.5 - x} \quad (45)$$

Proof: The proof is based on (42), where only the dominant term is kept. ■

This property shows a singularity of the derivative of $S_{x,0}$ near $x = 0.5$. However, one can also verify that under the condition of Property 11, the requirement $x \rightarrow 0.5$ means that $P_J \rightarrow \infty$ and $\rho \rightarrow 0$. So, (45) should be appreciated only under these asymptotical conditions. Clearly, for a fixed pair of P_J and ρ , (45) does not reflect the actual pattern of $S_{x,0}$ when x is so close to 0.5 that $(x, 0) \notin \mathcal{R}_\rho \cap \bar{\mathcal{R}}_\rho$ or $P_J \leq \max\{\gamma, \bar{\gamma}\}$, which will be further discussed later.

We now compare the secrecy between the left and right sides of Bob. At a Δ -distance to the left of Bob, $a = \frac{1}{(1-\Delta)^\alpha}$ and $b = \frac{1}{\Delta^\alpha}$. Under the condition of Property 11 with $\Delta \ll 1$ and hence $P_J \gg 1$ (but $\frac{P_T}{P_J}$ can be arbitrary), one can verify that $SNR_{A,E} = \Delta^\alpha (1 + \alpha\Delta) \frac{P_T}{P_J}$, $SNR_{B,E} = \Delta^{-\alpha} (1 - \alpha\Delta) \frac{P_T}{P_J}$ and hence

$$\begin{aligned} T_{0.5-\Delta,0} &= \left(1 + \Delta^\alpha (1 + \alpha\Delta) \frac{P_T}{P_J}\right) \left(1 + \Delta^{-\alpha} (1 - \alpha\Delta) \frac{P_T}{P_J}\right) \\ &= 1 + \Delta^{-\alpha} (1 - \alpha\Delta) \frac{P_T}{P_J} + (1 - \alpha^2 \Delta^2) \frac{P_T^2}{P_J^2} \end{aligned} \quad (46)$$

Similarly, at the same Δ -distance but to the right of Bob, one can verify that

$$T_{0.5+\Delta,0} = 1 + \Delta^{-\alpha} (1 + \alpha\Delta) \frac{P_T}{P_J} + (1 - \alpha^2 \Delta^2) \frac{P_T^2}{P_J^2} \quad (47)$$

¹⁶For compact expressions, we assume α is even.

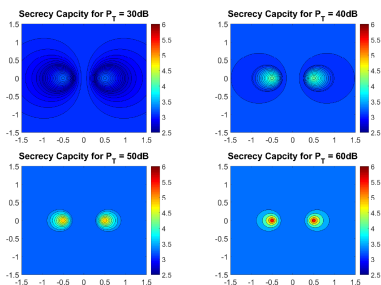


Fig. 14. “Flat near-field” with $P_J = \sqrt{\frac{P_T}{\rho}}$, $\alpha = 2$, $\rho = 0.1$ (i.e., $\log_2 \frac{1}{\rho} = 3.3$).

We see that $T_{0.5+\Delta,0} - T_{0.5-\Delta,0} = 2\alpha\Delta^{1-\alpha}\frac{P_T}{P_J} > 0$. It follows:

Property 14: Under the condition of Property 11, the secrecy capacity at a short distance to the right of Bob (or the left of Alice) is smaller than that at the same distance to the left of Bob (or the right of Alice).

The optimal jamming power to maximize $S_{x,y}$ is difficult to analyze in general due to the need to find the roots of a 4th-order polynomial in P_J . If we use the origin as the reference location, we know $S_{0,0} = S_{A,B,0,0} = S_{B,A,0,0}$ and hence $\arg \max_{P_J} S_{0,0} = \arg \max_{P_J} S_{A,B,0,0} = P_{J,opt,0,0}$ where $P_{J,opt,x,y}$ is given in (12). For small ρ and large P_T , one can verify that

$$P_{J,opt,0,0} = \sqrt{\frac{P_T}{\rho}} \quad (48)$$

Property 15: If $P_J = \sqrt{\frac{P_T}{\rho}}$ which is invariant to (x,y) , $\rho < \frac{\Delta^\alpha}{(1+\Delta)^\alpha}$, $1 > d_A > \Delta$, $1 > d_B > \Delta$, and $\Delta^\alpha \sqrt{\rho P_T} \gg 1$, then

$$S_{x,y} = \log_2 \frac{1}{\rho} \quad (49)$$

which is invariant to (x,y) .

Proof: It follows that $\frac{a}{b}\sqrt{\rho P_T} > \Delta^\alpha a\sqrt{\rho P_T} > \Delta^\alpha \sqrt{\rho P_T} \gg 1$ and $a\sqrt{\frac{P_T}{\rho}} > a\sqrt{\rho P_T} > \sqrt{\rho P_T} > \Delta^\alpha \sqrt{\rho P_T} \gg 1$. Similarly, $\frac{b}{a}\sqrt{\rho P_T} \gg 1$, $b\sqrt{\frac{P_T}{\rho}} \gg 1$ and $\sqrt{\rho P_T} \gg 1$. Then, one can verify that $S_{A,B,x,y} = \log_2 \frac{1}{\rho} - \log_2 \frac{a}{b} > 0$ and $S_{B,A,x,y} = \log_2 \frac{1}{\rho} - \log_2 \frac{b}{a} > 0$, which implies (49). ■

This property shows that under large P_T , small ρ and $P_J = \sqrt{\frac{P_T}{\rho}}$, there is a constant secrecy region in a “near-field”. But if $\sqrt{\rho P_T} \gg 1$ and Eve is far way from Alice and Bob, then one can verify that $S_{x,y} = \frac{1}{2} \log_2 \frac{P_T}{\rho}$, which is a constant secrecy in a “far-field” and as expected much larger than that in the near-field. Illustrated in Figs. 14 and 15 is the constant near-field secrecy capacity. We see that at $P_T = 60\text{dB}$, (49) is a good approximation of the near-field secrecy for both $\rho = 0.1$ and $\rho = 0.01$.

We now consider the case where (x,y) is so close to $(\pm 0.5, 0)$ that $(x,y) \notin \mathcal{R}_\rho \cap \bar{\mathcal{R}}_\rho$ or $P_J \leq \max\{\gamma, \bar{\gamma}\}$ (i.e., one of the conditions of Property of 11 is violated).

Property 16: Assume $\rho < \frac{1}{2^\alpha}$ so that \mathcal{R}_3 and $\bar{\mathcal{R}}_3$ do not exist, and \mathcal{R}_4 and $\bar{\mathcal{R}}_4$ are the complements of \mathcal{R}_ρ and $\bar{\mathcal{R}}_\rho$

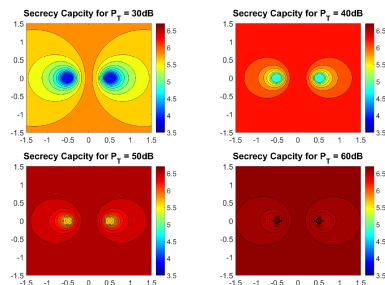


Fig. 15. “Flat near-field” with $P_J = \sqrt{\frac{P_T}{\rho}}$, $\alpha = 2$, $\rho = 0.01$ (i.e., $\log_2 \frac{1}{\rho} = 6.6$).

respectively. Recall $\mathcal{R}_{P_J} = \{(x,y) \in \mathcal{R}_\rho | P_J \leq \gamma\}$ and define $\bar{\mathcal{R}}_{P_J} = \{(x,y) \in \bar{\mathcal{R}}_\rho | P_J \leq \bar{\gamma}\}$. Then,

- 1) For $(x,y) \in \mathcal{R}_4 \cup \mathcal{R}_{P_J}$: $S_{x,y} = \frac{1}{2} S_{B,A,x,y}$ and, if $P_J > 0$, $\max_{x,y} S_{x,y} = S_{-0.5,0} = \frac{1}{2} \log_2(1 + SNR)$.
- 2) For $(x,y) \in \bar{\mathcal{R}}_4 \cup \bar{\mathcal{R}}_{P_J}$: $S_{x,y} = \frac{1}{2} S_{A,B,x,y}$ and, if $P_J > 0$, $\max_{x,y} S_{x,y} = S_{0.5,0} = \frac{1}{2} \log_2(1 + SNR)$.

Proof: First recall Property 4. Then consider that for $P_J > 0$, $SNR_{A,E}$ approaches zero as (x,y) approaches $(0.5, 0)$, and $SNR_{B,E}$ approaches zero as (x,y) approaches $(-0.5, 0)$. ■

This property says that with $P_J > 0$, $S_{x,y}$ actually peaks locally at the locations of Alice and Bob (although, under a large enough P_J , $S_{x,y}$ decreases as the location of Eve moves along the x -axis from the origin towards Alice or Bob initially when the condition of Property 11 holds). This property is clearly visible in Fig. 14, but is difficult to see in 15. The latter is because the regions $\mathcal{R}_4 \cup \mathcal{R}_{P_J}$ (around Alice) and $\bar{\mathcal{R}}_4 \cup \bar{\mathcal{R}}_{P_J}$ (around Bob) with $\rho = 0.01$ are too small within which the variation of $S_{x,y}$ is small.

B. With small-scale fading

With small-scale fading, the secrecy capacity is still given by (34) but with

$$SNR_{A,B} = \frac{\tilde{A}P_T}{1 + \rho\tilde{B}_1P_J} \quad (50)$$

$$SNR_{B,A} = \frac{\tilde{A}P_T}{1 + \rho\tilde{B}_2P_J} \quad (51)$$

$$SNR_{A,E} = \frac{a\tilde{C}P_T}{1 + b\tilde{D}P_J} \quad (52)$$

$$SNR_{B,E} = \frac{b\tilde{D}P_T}{1 + a\tilde{C}P_J} \quad (53)$$

where the small-scale fading factors are illustrated in Fig. 16. In particular, we assume that \tilde{A} is the same for either transmission from Alice to Bob or transmission from Bob to Alice (justified by the reciprocal property of electromagnetics). We treat \tilde{B}_1 and \tilde{B}_2 as different small-scale fading factors because the self-interference at Alice and that at Bob are affected differently by surrounding scattering objects due to the location difference of Alice and Bob. As in the previous section, we will assume that all small-scale fading factors are i.i.d. exponentially distributed with unit mean. Keep in

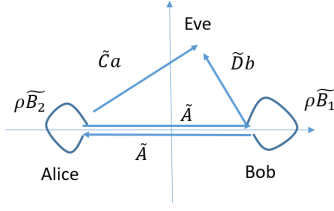


Fig. 16. Illustration of small-scale fading factors for fJam.

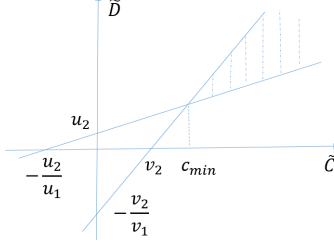


Fig. 17. Illustration of the integrated (shaded) area in (55).

mind that Alice and Bob can make decisions based on the knowledge of \tilde{A} , \tilde{B}_1 and \tilde{B}_2 .

It follows that $S_{x,y} = 0$ iff $C_{A,B} \leq C_{A,E}$ and $C_{B,A} \leq C_{B,E}$ or equivalently iff

$$\begin{cases} \tilde{C} - v_1\tilde{D} - v_2 \geq 0, \\ \tilde{D} - u_1\tilde{C} - u_2 \geq 0. \end{cases} \quad (54)$$

where $v_1 = \frac{b\tilde{A}P_J}{a(1+\rho\tilde{B}_1P_J)}$, $v_2 = \frac{\tilde{A}}{a(1+\rho\tilde{B}_1P_J)}$, $u_1 = \frac{a\tilde{A}P_J}{b(1+\rho\tilde{B}_2P_J)}$ and $u_2 = \frac{\tilde{A}}{b(1+\rho\tilde{B}_2P_J)}$. The pair of inequalities in (54) corresponds to the shaded area in Fig. 17. Then, the probability of zero secrecy conditional upon \tilde{A} , \tilde{B}_1 and \tilde{B}_2 is

$$\begin{aligned} \mathcal{P}_{\{S_{x,y}=0|\tilde{A},\tilde{B}_1,\tilde{B}_2\}} &= \int_{c_{min}}^{\infty} dx \int_{\frac{x-v_2}{v_1}}^{\infty} e^{-x-y} dy \\ &= \frac{1}{1+u_1} e^{-u_2-(1+u_1)c_{min}} - \frac{1}{1+\frac{1}{v_1}} e^{\frac{v_2}{v_1}-(1+\frac{1}{v_1})c_{min}} \end{aligned} \quad (55)$$

where

$$c_{min} = \begin{cases} \frac{v_2+v_1u_2}{1-v_1u_1}, & v_1u_1 < 1 \\ \infty & \text{otherwise} \end{cases} \quad (56)$$

One can further verify from (17) and (56) that

$$\mathcal{P}_{\{S_{x,y}=0|\tilde{A},\tilde{B}_1,\tilde{B}_2\}} = \begin{cases} Ke^{-E}, & w_1 > 0 \\ 0 & \text{otherwise} \end{cases} \quad (57)$$

where $K = \frac{w_1}{w_2}$, $E = \frac{w_3}{w_1}$ and

$$w_1 = ab[(1+\rho\tilde{B}_1P_J)(1+\rho\tilde{B}_2P_J) - \tilde{A}^2P_J^2] \quad (58)$$

$$w_2 = [a\tilde{A}P_J + b(1+\rho\tilde{B}_2P_J)][b\tilde{A}P_J + a(1+\rho\tilde{B}_1P_J)] \quad (59)$$

$$w_3 = \tilde{A}[a(1+\rho\tilde{B}_1P_J) + b(1+\rho\tilde{B}_2P_J) + b\tilde{A}P_J + a\tilde{A}P_J] \quad (60)$$

Property 17: With zero jamming power, the unconditional probability of zero secrecy anywhere is upper bounded by that at origin, i.e.,

$$\mathcal{P}_{\{S_{x,y}=0|P_J=0\}} \leq \mathcal{P}_{\{S_{0,0}=0|P_J=0\}} = \frac{1}{1+0.5^{\alpha-1}} \quad (61)$$

Also, for an Eve arbitrarily close to Alice or Bob, we have $\mathcal{P}_{\{S_{\pm 0.5,0}=0|P_J=0\}} = 0.5$.

Proof: If $P_J = 0$, then $K = 1$ and $E = \tilde{A}\frac{a+b}{ab}$. Hence $\mathcal{P}_{\{S_{x,y}=0|P_J=0\}} = \mathcal{E}\{\mathcal{P}_{\{S_{x,y}=0|\tilde{A},\tilde{B}_1,\tilde{B}_2,P_J=0\}}\} = \mathcal{E}\{e^{-\tilde{A}\frac{a+b}{ab}}\} = \frac{1}{1+\frac{a+b}{ab}}$. Given a , $\frac{a+b}{ab}$ is a decreasing function of b . So, for any given d_A , $\max_{x,y} \mathcal{P}_{\{S_{x,y}=0|P_J=0\}}$ is achieved by the smallest d_B . So, $\max_{x,y} \mathcal{P}_{\{S_{x,y}=0|P_J=0\}}$ is achieved only if $y = 0$. Now consider $y = 0$ and $\mathcal{P}_{\{S_{x,0}=0|P_J=0\}} = \frac{1}{1+|x+0.5|^{\alpha}+|x-0.5|^{\alpha}}$ which is symmetric of x and has its peak at $x = 0$. And obviously $\mathcal{P}_{\{S_{\pm 0.5,0}=0|P_J=0\}} = 0.5$. ■

If $P_J = \infty$,

$$K = \frac{ab(\rho^2\tilde{B}_1\tilde{B}_2 - \tilde{A}^2)}{(a\tilde{A} + \rho b\tilde{B}_2)(b\tilde{A} + \rho a\tilde{B}_1)} \quad (62)$$

$$E = \frac{\tilde{A}(\rho a\tilde{B}_1 + \rho b\tilde{B}_2 + b\tilde{A} + a\tilde{A})}{ab(\rho^2\tilde{B}_1\tilde{B}_2 - \tilde{A}^2)P_J} \rightarrow 0 \quad (63)$$

Hence,

$$\begin{aligned} \mathcal{P}_{\{S_{x,y}=0|P_J=\infty\}} &= \mathcal{E}\{K\} \\ &= \int_0^{\infty} \int_0^{\infty} \int_0^{\rho\sqrt{uv}} Ke^{-u-v-w} dudvdw \end{aligned} \quad (64)$$

where the random variables $\tilde{A}, \tilde{B}_1, \tilde{B}_2$ in K should be replaced by the dummy variables w, u, v respectively (this rule will be used again later). Note that $\arg \max_{x,y} K$ is generally a function of \tilde{A}, \tilde{B}_1 and \tilde{B}_2 . Unlike the case of $P_J = 0$, it seems intractable to find an analytical form of $\arg \max_{x,y} \mathcal{P}_{\{S_{x,y}=0|P_J=\infty\}}$.

For the general case of $P_J > 0$, searching for the worst location of Eve in terms of $\mathcal{P}_{\{S_{x,y}=0|\tilde{A},\tilde{B}_1,\tilde{B}_2\}}$ or $\mathcal{P}_{\{S_{x,y}=0\}}$ is also hard. But the following special case should be of interest:

Property 18: If $P_J > 0$ and Eve is arbitrarily close to Alice or Bob, then the probability of zero secrecy is zero, i.e., $\mathcal{P}_{\{S_{\pm 0.5,0}=0|P_J>0\}} = 0$.

Proof: Assume any $P_J > 0$. At $(x, y) = (0.5, 0)$, we have $a = 1$ and $b = \infty$, and hence $v_1 = \infty$, $v_2 = \frac{\tilde{A}}{1+\rho\tilde{B}_1P_J}$, $u_1 = 0$ and $u_2 = 0$. In this case, v_1u_1 is not defined and the previous derivation does not apply. To see the corresponding result, we consider the necessary condition for zero secrecy: $C - v_1D - v_2 \geq 0$, which now holds with zero probability (since $v_1 = \infty$). Hence, $\mathcal{P}_{\{S_{\pm 0.5,0}=0|\tilde{A},\tilde{B}_1,\tilde{B}_2,P_J>0\}} = 0$ and hence $\mathcal{P}_{\{S_{\pm 0.5,0}=0|P_J>0\}} = 0$. ■

Property 18 is in contrast to the case of colluding Eves where the probability of zero secrecy at Alice is always one. See Part 3 in Property 8.

Property 19: iff $\tilde{A}^2 > \rho^2\tilde{B}_1\tilde{B}_2$: then there is a $P_J^* > 0$ such that iff $P_J \geq P_J^*$, $\mathcal{P}_{\{S_{x,y}=0|\tilde{A},\tilde{B}_1,\tilde{B}_2\}} = 0$, where

$$P_J^* = \frac{\rho(\tilde{B}_1 + \tilde{B}_2) + \sqrt{\rho^2(\tilde{B}_1 + \tilde{B}_2)^2 + 4(\tilde{A}^2 - \rho^2\tilde{B}_1\tilde{B}_2)}}{2(\tilde{A}^2 - \rho^2\tilde{B}_1\tilde{B}_2)} \quad (65)$$

Namely, iff $\tilde{A}^2 > \rho^2\tilde{B}_1\tilde{B}_2$, Alice and Bob can choose a P_J to make the probability of zero secrecy equal to zero anywhere.

Proof: The proof follows from (57) and (58). ■

Property 19 can be used for dynamic control of jamming power. A semi-dynamic control is: Alice and Bob choose $P_J = P_J^*$ if $\tilde{A}^2 > \rho^2\tilde{B}_1\tilde{B}_2$, or a constant P_J if $\tilde{A}^2 \leq \rho^2\tilde{B}_1\tilde{B}_2$.

Property 20: With the above semi-dynamic control of jamming power, we have

$$\mathcal{P}_{\{S_{x,y}=0\}} = \int_0^\infty \int_0^\infty \int_0^{\rho\sqrt{uv}} K e^{-E} e^{-u-v-w} dudvdw < \mathcal{P}_1 \quad (66)$$

with $\mathcal{P}_1 = \text{Prob}\{\tilde{A}^2 \leq \rho^2 \tilde{B}_1 \tilde{B}_2\}$, i.e.,

$$\mathcal{P}_1 = \int_0^\infty \int_0^\infty e^{-u-v} [1 - e^{-\rho\sqrt{uv}}] dudv < \frac{\pi\rho}{4} \quad (67)$$

where the last inequality becomes tight as ρ becomes small.

Proof: $\mathcal{P}_{\{S_{x,y}=0\}}$ is the expectation of $\mathcal{P}_{\{S_{x,y}=0|\tilde{A},\tilde{B}_1,\tilde{B}_2\}}$ in (57) subject to $\tilde{A}^2 \leq \rho^2 \tilde{B}_1 \tilde{B}_2$. Using $K e^{-E} < 1$, we have

$$\begin{aligned} \mathcal{P}_{\{S_{x,y}=0\}} &< \mathcal{P}_1 \doteq \int_0^\infty \int_0^\infty \int_0^{\rho\sqrt{uv}} e^{-u-v-w} dudvdw \\ &= \int_0^\infty \int_0^\infty e^{-u-v} [1 - e^{-\rho\sqrt{uv}}] dudv \\ &< \int_0^\infty \int_0^\infty e^{-u-v} \rho\sqrt{uv} dudv = \frac{\pi\rho}{4} \end{aligned} \quad (68)$$

where the second inequality is due to $1 - e^{-z} < z$ for any $z > 0$, and the last equality follows from the fact $\int_0^\infty e^{-u} \sqrt{u} du = \frac{\sqrt{\pi}}{2}$. This fact can be proved by using the change of variable $u = \frac{v^2}{2}$, which leads to $\int_0^\infty e^{-u} \sqrt{u} du = \frac{\sqrt{\pi}}{2} \sigma^2$ where $\sigma^2 = \frac{2}{\sqrt{2\pi}} \int_0^\infty v^2 e^{-\frac{v^2}{2}} dv = 1$ which is known as the variance of a Gaussian random variable with zero mean and unit variance. ■

Property 21: If P_J is a constant regardless of $\tilde{A}^2 > \rho^2 \tilde{B}_1 \tilde{B}_2$, then

$$\mathcal{P}_{\{S_{x,y}=0\}} = \int_0^\infty \int_0^\infty \int_0^{w_0} K e^{-E} e^{-u-v-w} dudvdw < \mathcal{P}_2 \quad (69)$$

where $w_0 = \sqrt{\rho^2 uv + \frac{1+\rho(u+v)P_J}{P_J^2}}$ and

$$\mathcal{P}_2 = \int_0^\infty \int_0^\infty e^{-u-v} [1 - e^{-w_0}] dudv > \mathcal{P}_1 \quad (70)$$

and for $P_J = \infty$, $\mathcal{P}_1 = \mathcal{P}_2$.

Proof: Similar to the proof of Property 20. ■

Illustrated in Fig. 18 are the probabilities shown in Properties 20 and 21. We see that the benefit from the semi-dynamic jamming power control is significant when P_J is small. But when P_J is large, the benefit diminishes.

In scattering-rich environment, if Alice and Bob both move in random directions with a distance in the order of half-wavelength, all of \tilde{A} , \tilde{B}_1 and \tilde{B}_2 could change substantially and independently. In MANET, Alice and Bob could move around and do not exchange any secret key till they find $\tilde{A}^2 > \rho^2 \tilde{B}_1 \tilde{B}_2$, and only then they exchange secret keys with $P_J = P_J^*$. We call this a full-dynamic control of jamming power, for which the probability of zero secrecy is simply zero. Compared to the semi-dynamic control, the full-dynamic control has a larger latency and also potentially consumes more jamming power. Also note that the probability for the condition $\tilde{A}^2 > \rho^2 \tilde{B}_1 \tilde{B}_2$ to hold is $1 - \mathcal{P}_1 > 1 - \frac{\pi\rho}{4}$. So, if ρ is small, Alice and Bob will find that condition satisfied frequently.

Alternatively, if P_J is limited, Alice and Bob can wait till $\mathcal{P}_{\{S_{x,y}=0|\tilde{A},\tilde{B}_1,\tilde{B}_2\}}$ shown in (55) at a worst location of Eve is

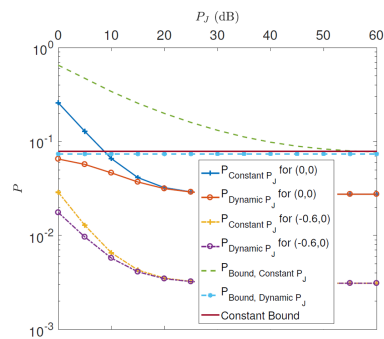


Fig. 18. Probabilities shown in Properties 20 and 21 where $\alpha = 2$, $\rho = 0.1$. The “constant bound” is $\frac{\pi\rho}{4}$. The meanings of other symbols should be self-evident. For location-dependent probabilities, we choose $(x, y) = (0, 0)$ and $(x, y) = (-0.6, 0)$.

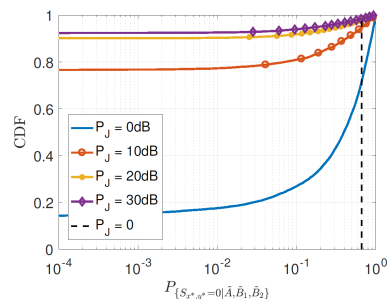


Fig. 19. CDF of $\mathcal{P}_{\{S_{x,y}=0|\tilde{A},\tilde{B}_1,\tilde{B}_2\}}$ with $\alpha = 2$, $\rho = 0.1$ and $(x, y) = (0, 0)$.

small enough (instead of zero). We call this a general-dynamic control. Shown in Fig. 19 are the CDFs of $\mathcal{P}_{\{S_{x,y}=0|\tilde{A},\tilde{B}_1,\tilde{B}_2\}}$ at $x = y = 0$, based on 10000 realizations of \tilde{A} , \tilde{B}_1 , \tilde{B}_2 . We see that even when P_J is only zero dB (i.e., equal to the variance of the background noise), there is more than 10% chance that $\mathcal{P}_{\{S_{x,y}=0|\tilde{A},\tilde{B}_1,\tilde{B}_2\}}$ is less than 10^{-4} . These CDFs should have a direct impact on the latency of the general-dynamic control.

Property 22: If $P_J = \sqrt{\frac{P_T}{\rho}}$ which is invariant to (x, y) , $\rho < \frac{\Delta^\alpha}{(1+\Delta)^\alpha}$, $1 > d_A > \Delta$, $1 > d_B > \Delta$, and $\Delta^\alpha \sqrt{\rho P_T} \gg 1$, then with a high probability,

$$S_{x,y} \approx \log_2 \frac{\tilde{A}}{\rho \sqrt{\tilde{B}_1 \tilde{B}_2}} \quad (71)$$

which is invariant to (x, y) . And under the above conditions,

$$\text{Prob}\{S_{x,y} \leq s\} < \frac{2^s \rho \pi}{4} \quad (72)$$

Proof: Proof of (71) is similar to that of Property 15. Proof of (72) is similar to that of (68). ■

The result (71) says that under a large P_T , a small ρ and $P_J = \sqrt{\frac{P_T}{\rho}}$, there is a constant near-field secrecy capacity conditional upon \tilde{A} , \tilde{B}_1 and \tilde{B}_2 . Illustrated in Figs. 20 and 21 is $S_{x,y}$ versus (x, y) in the near-field subject to $\tilde{A} = \tilde{B}_1 = \tilde{B}_2 = 1$ where \tilde{C} and \tilde{D} change randomly and independently as (x, y) changes (with step size equal to 0.01 in each direction). As predicted by Property 22, we see that

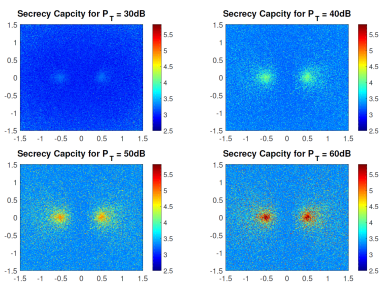


Fig. 20. With small-scale fading and subject to $\tilde{A} = \tilde{B}_1 = \tilde{B}_2 = 1$, $S_{x,y}$ vs (x, y) . For each (x, y) , there is a new realization of \tilde{C} and \tilde{D} . $\alpha = 2$, $\rho = 0.1$, $P_J = \sqrt{\frac{P_T}{\rho}}$.

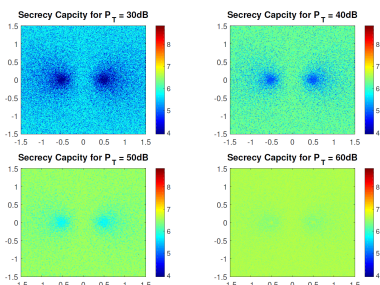


Fig. 21. With small-scale fading and subject to $\tilde{A} = \tilde{B}_1 = \tilde{B}_2 = 1$, $S_{x,y}$ vs (x, y) . For each (x, y) , there is a new realization of \tilde{C} and \tilde{D} . $\alpha = 2$, $\rho = 0.01$, $P_J = \sqrt{\frac{P_T}{\rho}}$.

with $P_T = 60dB$ and $\rho = 0.01$, there is very little variation in the near-field distribution of $S_{x,y}$.

Since $S_{x,y}$ in (71) still depends on \tilde{A} , \tilde{B}_1 and \tilde{B}_2 , Alice and Bob could ideally wait till $\frac{\tilde{A}}{\sqrt{\tilde{B}_1 \tilde{B}_2}}$ is maximized before exchanging any keys. This is however not possible due to non-causality in knowing the future realizations of small-scale fading. In practice, Alice and Bob should only wait until $\log_2 \frac{\tilde{A}}{\rho \sqrt{\tilde{B}_1 \tilde{B}_2}}$ is a large enough positive number. The result in (72) provides an upper bound on the probability that $\log_2 \frac{\tilde{A}}{\rho \sqrt{\tilde{B}_1 \tilde{B}_2}}$ is no larger than a pre-specified value s of secrecy. Obviously, this upper bound on the right side of (72) can be made small if ρ is small enough. It is equivalent to write (72) as $Prob\{S_{x,y} > s\} > 1 - \frac{2^s \rho \pi}{4}$, which quantifies how to make the constant near-field secrecy capacity larger than a pre-specified value s with high probability by choosing a small enough normalized self-interference channel gain ρ . Remember that under a fixed actual self-interference channel gain ρ' , the value of ρ can be controlled by controlling the actual distance (or actual channel gain) between Alice and Bob. Such a control is feasible in mobile wireless networks.

V. FINAL REMARKS

Full-duplex radio is an emerging wireless communication technology with many potential applications. This paper addresses its use for secure wireless communication. Unlike many previous works for this purpose, we have examined the fundamental properties of full-duplex radio for secure wireless communication where the legitimate users have virtually zero

knowledge of the channel state information of eavesdroppers. Among the important findings are how the secrecy capacity of a link between two single-antenna radios is distributed in space with or without collusion among eavesdroppers, how the residual self-interference channel gain of full-duplex radio affects the distribution of the secrecy capacity, and how the small-scale fading affects the probabilities of zero (or positive) secrecy. All of the major findings have been quantified precisely and stated in a list of properties. Some of these properties might not be surprising to some experts in this area. But to our knowledge, none of these properties is readily available elsewhere (from other authors). Indeed we hope that all of them are original and insightful. We also hope that this work will be useful for helping real-world applications and more importantly for inspiring further research in understanding the limits and potentials of full-duplex radio for secure wireless communication in more advanced network settings.

REFERENCES

- [1] N. Ferguson, B. Schneier, and T. Kohno, *Cryptography Engineering*. Hoboken, NJ, USA: Wiley, 2010.
- [2] A. Mukherjee, S. A. A. Fakoorian, J. Huang, and A. L. Swindlehurst, "Principles of physical layer security in multiuser wireless networks: A survey," *IEEE Commun. Surveys Tuts.*, vol. 16, no. 3, pp. 1550-1573, 3rd Quart., 2014.
- [3] Y. Zou, J. Zhu, X. Wang, and L. Hanzo, "A Survey on Wireless Security: Technical Challenges, Recent Advances, and Future Trends," *Proceedings of the IEEE*, Vol. 104, No. 9, September 2016.
- [4] H. Krishnaswamy and G. Zussman, "1 chip 2x the bandwidth," *IEEE Spectr.*, vol. 53, no. 7, pp. 38-54, Jul. 2016.
- [5] L. Chen, Q. Zhu, W. Meng and Y. Hua, "Fast power allocation for secure communication with full-duplex radio", *IEEE Transactions on Signal Processing*, Vol. 65, No. 14, pp. 3846-3861, July 2017.
- [6] T.-X. Zheng, H.-M. Wang, Q. Yang, and M. H. Lee, "Safeguarding decentralized wireless networks using full-duplex jamming receivers", *IEEE Transactions on Wireless Comm.*, Vol. 16, No. 1, Jan. 2017.
- [7] M. R. Abedi, N. Mokari, H. Saeedi, and H. Yanikomeroglu, "Robust resource allocation to enhance physical layer security in systems with full-duplex receivers: Active adversary", *IEEE Transactions on Wireless Comm.*, Vol. 16, No. 2, Feb 2017.
- [8] X. Tang, P. Ren, Y. Wang, and Z. Han, "Combating full-duplex active eavesdropper: A hierarchical game perspective", *IEEE Trans. on Comm.*, Vol. 65, No. 3, Mar 2017.
- [9] B. Akgun, O. O. Koyluoglu, and M. Krunz, "Exploiting full-duplex receivers for achieving secret communications in multiuser MISO networks," *IEEE Trans. on Comm.*, Vol. 65, No. 2, Feb 2017.
- [10] G. Zheng, I. Krikidis, J. Li, A. P. Petropulu, and B. Ottersten, "Improving physical layer secrecy using full-duplex jamming receivers," *IEEE Trans. Signal Process.*, vol. 61, no. 20, pp. 4962-4974, Oct. 2013.
- [11] D. Tse and P. Viswanath, *Fundamentals of Wireless Communication*, Cambridge University Press, 2005.
- [12] Y. Hua, Y. Ma, A. Gholian, Y. Li, A. Ciric, P. Liang, "Radio self-interference cancellation by transmit beamforming, all-analog cancellation and blind digital tuning," *Signal Processing*, Vol. 108, pp. 322-340, 2015.
- [13] S. Gollakota and D. Katabi, "Physical layer wireless security made fast and channel independent," *INFOCOM*, 2011.